Supplementary Materials for

Active DNA Demethylation in Plant Companion Cells Reinforces Transposon Methylation in Gametes

Christian A. Ibarra, Xiaoqi Feng, Vera K. Schoft, Tzung-Fu Hsieh, Rie Uzawa, Jessica A. Rodrigues, Assaf Zemach, Nina Chumak, Adriana Machlicova, Toshiro Nishimura, Denisse Rojas, Robert L. Fischer, Hisashi Tamaru, Daniel Zilberman

*To whom correspondence should be addressed. E-mail: rfischer@berkeley.edu (R.L.F.); hisashi.tamaru@gmi.oeaw.ac.at (H.T.); danielz@berkeley.edu (D.Z.)

Published 14 September 2012, *Science* **337**, 1360 (2012)
DOI: 10.1126/science.1224839

This PDF file includes:

Materials and methods

Isolation of *A. thaliana* endosperm. Stage 12-13 flower buds were emasculated and pollinated 48 hours later. Reciprocal crosses were performed using wild-type Col-0 and L*er* ecotypes. In addition, *dme-2* (Col-*gl*) (*16*) heterozygous flowers were pollinated with wild-type (L*er*) pollen, and *fie-1* (L*er*) (*17*) heterozygous flowers were pollinated with wild-type (Col-0) pollen. For wild-type crosses, seven to eight days after pollination, F1 seeds (torpedo-stage to early-bent-cotyledon stage) were immersed in 0.3 M sorbitol and 5 mM Mes (pH 5.7) on a slide under a dissecting microscope. Embryo and endosperm were dissected using a fine needle and forceps. The seed coat was discarded. Wild-type embryos were twice centrifuged and the pellet resuspended in 0.3 M sorbitol and 5 mM Mes (pH 5.7) to remove contaminating endosperm. For crosses with the *dme-2* or *fie-1* mutations, F1 aborting seeds were identified and mutant endosperm was isolated. Approximately 500 wild-type endosperm, 1000 *dme-2* or *fie-1* endosperm, and 300 wild-type embryos were collected.

Isolation of vegetative cell and sperm nuclei. Pollen was isolated from wild-type (Col-0) and *dme-2* heterozygous plants (Col-*gl* ecotype) as described previously (*8, 9*). Vegetative cell and sperm nuclei were extracted from mature pollen and fractionated by fluorescence activated cell sorting as described previously (*8, 9*).

Bisulfite sequencing library construction. As described previously, genomic DNA was isolated from vegetative cell and sperm nuclei (*8*), endosperm, and embryo (*3*). Paired-end bisulfite sequencing libraries for Illumina sequencing were constructed as described previously (*3*) with minor modifications. In brief, about 150 ng of genomic DNA was fragmented by sonication, end repaired and ligated to custom-synthesized methylated adapters (Eurofins MWG Operon) according to the manufacturer's (Illumina) instructions for gDNA library construction. Adaptor-ligated libraries were subjected to two successive treatments of sodium bisulfite conversion using the EpiTect Bisulfite kit (Qiagen) as outlined in the manufacturer's instructions. One quarter of the bisulfite-converted libraries was PCR amplified using the following conditions: 2.5 U of ExTaq DNA polymerase (Takara Bio), 5 µl of 10X Extaq reaction buffer, 25 µM dNTPs, 1 µl Primer 1.1, 1 µl Primer 2.1 (50 µl final). PCR reactions were carried out as follows: 95ºC 3 min, then 12-14 cycles of 95ºC 30 sec, 65ºC 30 sec and 72ºC 60 sec. The enriched libraries were purified twice with solid phase reversible immobilization (SPRI) method using AM-Pure beads (Beckman Coulter) prior to quantification with a Bioanalyzer (Agilent). Sequencing on the Illumina platform was performed at the Vincent J. Coates Genomic Sequencing Laboratory at UC Berkeley and the Genome Center at UC Davis.

Allele-specific determination of DNA methylation. Reads were sorted to the Col and L*er* genomes as described (*4*). DNA methylation of cytosines within sorted reads was calculated as described (*3, 18*).

Gene and TE meta analysis (ends analysis). *A. thaliana* TAIR-annotated genes or transposons were aligned at the 5' end or the 3' end. For genes and TEs, we discarded from the analysis 1500 bp or 250 bp, respectively, from the end opposite to the one used for alignment to avoid averaging the edges of shorter genes and TEs with the middles of longer sequences.

Density plots. All DNA methylation kernel density plots compare fractional methylation within 50-bp windows. We used windows with at least 20 informative sequenced cytosines (10 for

CHG in endosperm) and fractional methylation of at least 0.7 (CG), 0.4 (CHG endosperm), 0.5 (CHG pollen), 0.08 (CHH endosperm), 0.15 (CHH vegetative cell), or 0.05 (CHH sperm) in at least one of the samples being compared. For parent-of-origin endosperm plots, only windows with methylation differences between Col and L*er* below 0.1 (CG), 0.15 (CHG), or 0.05 (CHH) were used to exclude ecotype-specific differences. Windows in which fractional paternal (or sperm) CG methylation exceeded fractional maternal (or vegetative cell) CG methylation by at least 0.4 were considered demethylated.

Box plots. Box plots compare fractional methylation in TEs within 50-bp windows and use the same cutoffs as density plots. To examine the correlation between CG demethylation and chromatin structure, TE windows are separated into five groups in ascending order according to GC ratio, nucleosome enrichment, dimethylation of lysine 9 of histone H3 (H3K9me2), and distance from the closest edge of the TE, respectively. The five groups are as follows: for GC ratio, 0.2-0.3, 0.3-0.35, 0.35-0.4, 0.4-0.45, and >0.45; for nucleosome enrichment, 1-8, 9-16, 17-24, 25-39, and >39 counts (*19*); for H3K9me2, <0.5, 0.5-1.25, 1.25-2, 2-3, and >3 $\log_2$ (IP/input) (*20*); for distance to TE edge, <50 bp, 50-100 bp, 100-150 bp, 150-200 bp, and 200-250 bp.

Correlation with histone modifications. Spearman correlation coefficients between TE methylation changes and histone modifications were calculated using 50-bp windows. Data for nucleosomes were derived from (*19*); for H3K9me2 from (*20*); for H3K27me3 from (*21*), and for all other histone modifications from (*10*).

Identification of DMRs and overlaps with imprinted loci. Fractional CG methylation in 50-bp windows across the genome was compared between *dme* endosperm and wild-type endosperm and also between the sperm cell and vegetative cell. Windows with a fractional CG methylation difference of at least 0.3 in the endosperm comparison (Fisher's exact test p-value < 0.001) and at least 0.5 in the vegetative cell comparison (Fisher's exact test p-value < 10^{-10}) were merged to generate larger differentially methylated regions (DMRs) if they occurred within 300 bp. DMRs were retained for further analysis if the fractional CG methylation across the whole DMR was 0.3 greater in *dme* endosperm than in wild-type endosperm or 0.5 greater in the sperm cell than in the vegetative cell (Fisher's exact test p-value < 10^{-10} in both cases), and if the DMR was at least 100 bp. We thus generated 9,816 endosperm DMRs and 9,932 pollen DMRs.

The list of *A. thaliana* imprinted genes was obtained by combining the 114 maternally expressed genes and 9 paternally expressed genes from (*4*), 39 maternally expressed genes and 27 paternally expressed genes from (*22*) and 165 maternally expressed genes and 43 paternally expressed genes from (*23*). DMR distribution with respect to imprinted genes is shown in fig. S7.

Artificial microRNA transgene construction and analysis. We used the *AGL61* promoter to express an artificial microRNA directed against the *GFP* transcript specifically in the central cell (*24*). The *AGL61* promoter was PCR amplified from Col-0 genomic DNA using the primers AGL61F-salI (5'-TGATTACGCCGTCGACAGATGATTTTAGAGTCTCCCGC-3') and AGL61R-asc1 (5'- CTCACCATGGCGCGCCTGTAACATACATTTGTAATTACTCG-3'). The *AGL61* promoter was then cloned into the *LAT52p-amiRNA=GFP* plasmid described in (*7*), replacing the *LAT52* promoter at the SalI and AscI sites to create the *AGL61p-amiRNA=GFP* transgene. As a negative control, the *amiRNA-GFP* fragment was removed by EcoRI digestion followed by self-ligation of the remaining plasmid to create the *AGL61p* transgene. As a positive control, we used the *DD45* promoter to express an artificial microRNA directed against the *GFP*

transcript specifically in the egg cell (*25*). The *DD45* promoter was amplified from Col-0 genomic DNA using primers DD45F-SalI (5'-GACTGTCGACTAAATGTTCCTCGCTGACGT-3') and DD45R-AscI (5'-CTAGGCGCGCCTGTGTTAGAAGCCATTATTC-3'). The DD45 promoter was inserted into the *LAT52p-amiRNA=GFP* plasmid, replacing the *LAT52* promoter at the SalI and AscI sites to create the *DD45p-amiRNA=GFP* transgene.

Transgenic lines and microscopy analysis. Using Agrobacterium-mediated floral dip transformation (*26*), the *AGL61p-amiRNA=GFP*, *AGL61p*, or *DD45p-amiRNA=GFP* transgenes were transformed into a *DD45p-GFP* homozygous reporter line that expresses GFP specifically in the egg cell (*25*). Transgenic seeds were selected on plates with hygromycin antibiotic. PCR procedures were used to detect the presence of the *AGL61p-amiRNA=GFP*, *AGL61p*, or *DD45p-amiRNA=GFP* transgenes as well as the *DD45p-GFP* reporter transgene in hygromycin-resistant T1 seedlings. We monitored the intensity of GFP fluorescence in T1 plants. Anthers were removed from stage 12 to 13 flower buds to prevent fertilization (*27*). Carpels were dissected 48 hours later and GFP fluorescence in intact unfertilized ovules was observed as described previously (*28*). GFP intensity was visually scored and grouped into two categories: strong GFP fluorescence versus faint or no GFP fluorescence. Resistance to hygromycin antibiotic was used to genotype plants for the *AGL61p-amiRNA=GFP* transgene.

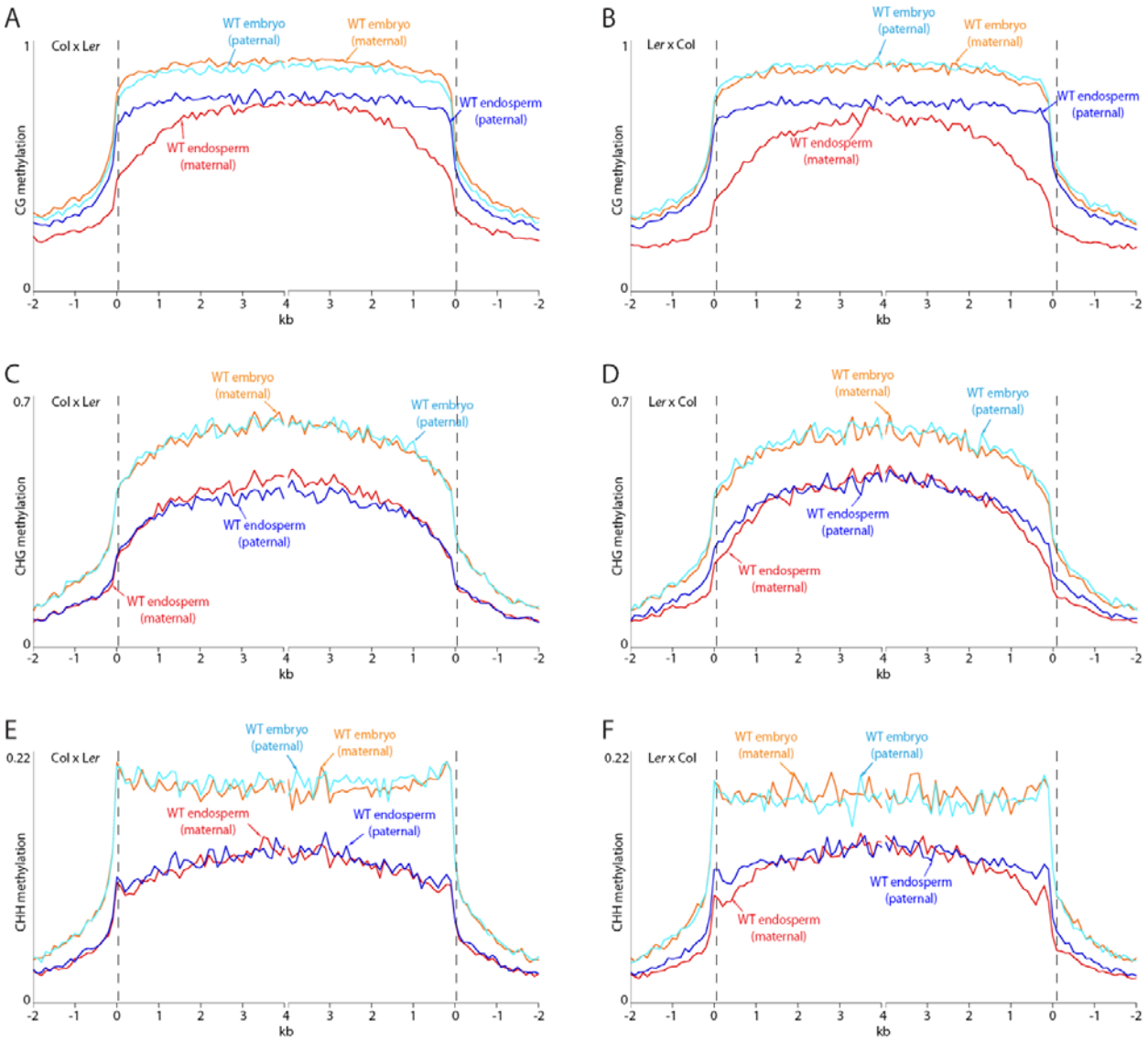

Fig. S1. DNA methylation of transposons in *A. thaliana* seed. (**A-F**) *A. thaliana* transposons were aligned at the 5' end (left panel) or the 3' end (right panel) and average methylation levels for each 100-bp interval are plotted for endosperm and embryo derived from Col x L*er* F1 seeds (**A, C, E**) and L*er* x Col F1 seeds (**B, D, F**). The dashed line at zero represents the point of alignment. CG methylation is shown in (**A-B**), CHG in (**C-D**), CHH in (**E-F**).

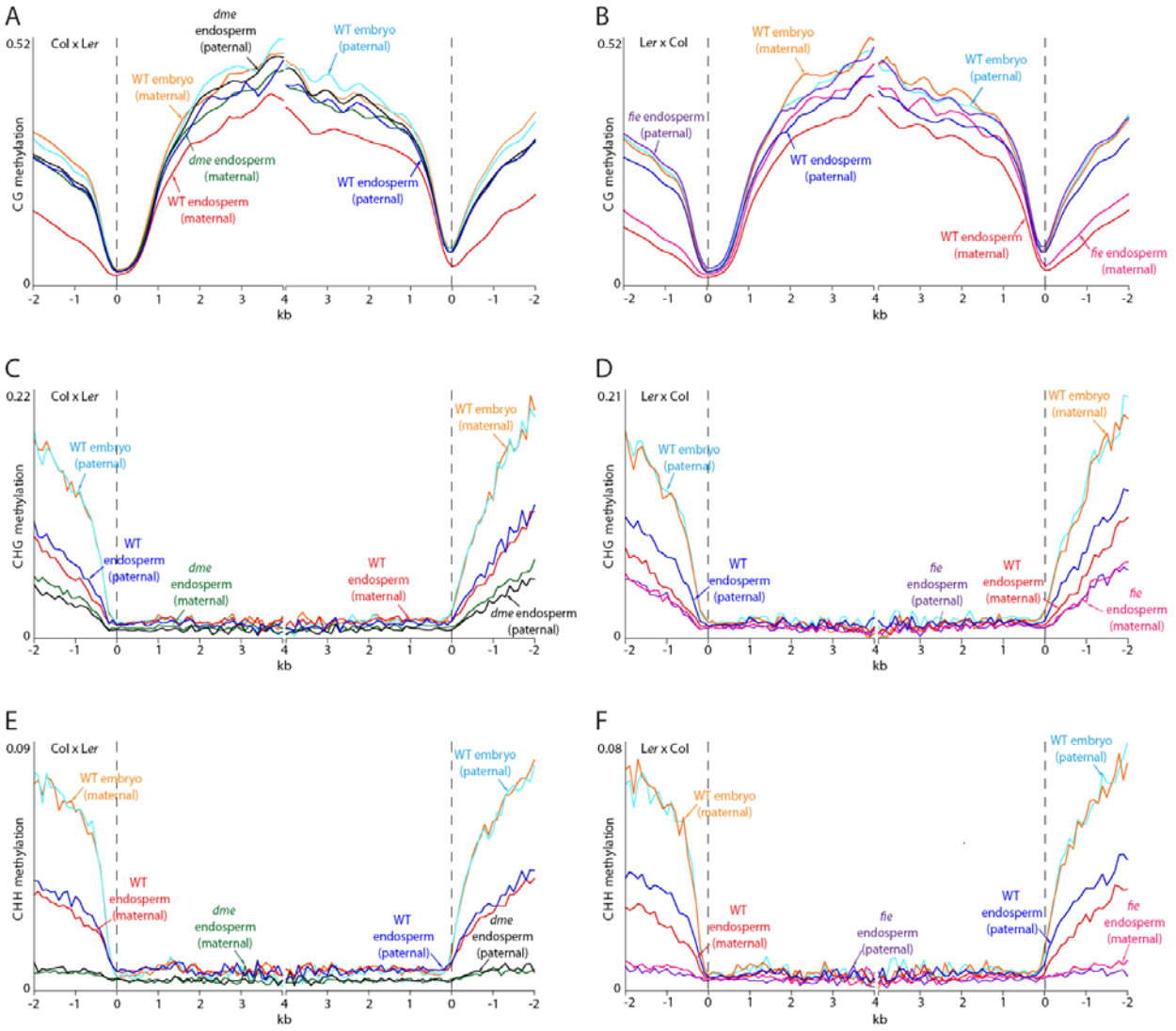

Fig. S2. DNA methylation of genes in the seed. (**A-F**) *A. thaliana* genes were aligned at the 5' end (left panel) or the 3' end (right panel) and average methylation levels for each 100-bp interval are plotted for endosperm derived from Col x L*er* and *dme-2* (Col) x L*er* F1 seeds, and embryo derived from Col x L*er* seeds (**A, C, E**), and for endosperm derived from L*er* x Col and *fie-1* (L*er*) x Col F1 seeds, and embryo derived from L*er* x Col seeds (**B, D, F**). The dashed line at zero represents the point of alignment. CG methylation is shown in (**A-B**), CHG in (**C-D**), CHH in (**E-F**).

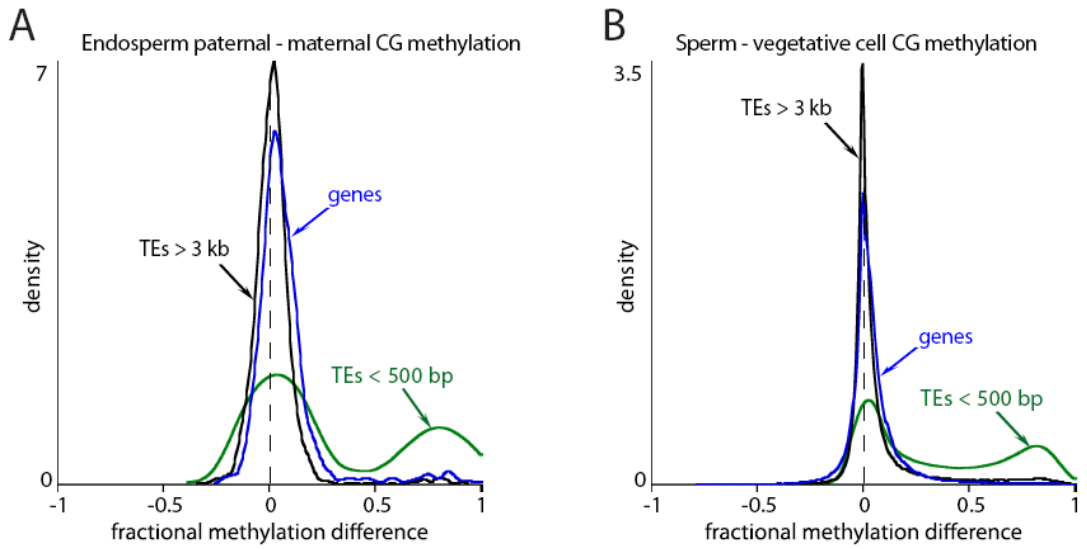

Fig. S3. Maternal demethylation in genes and transposons (TEs). (**A**-**B**) Kernel density plots trace the frequency distribution of the differences between *A. thaliana* paternal and maternal endosperm CG methylation (**A**), and sperm and vegetative cell CG methylation (**B**).

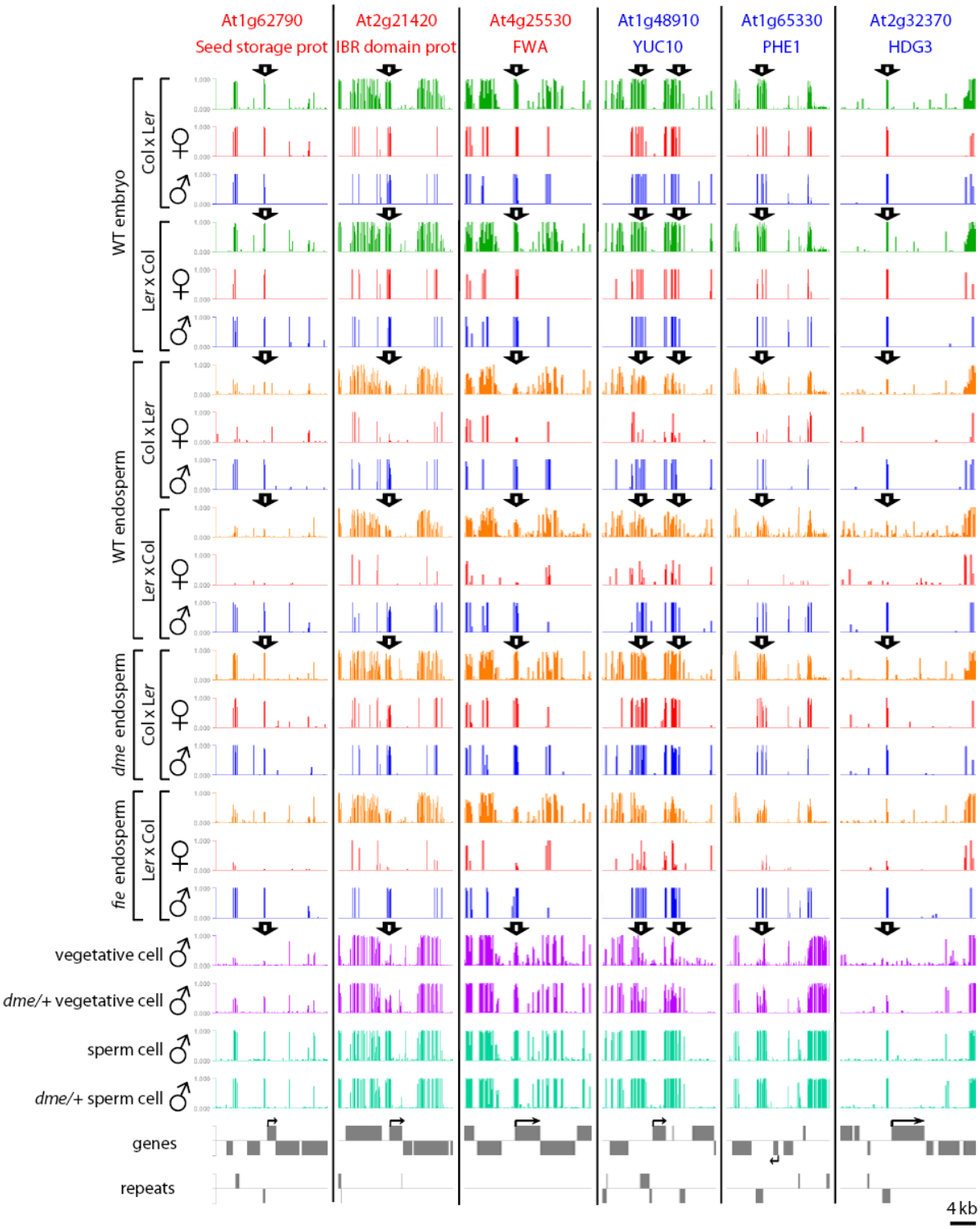

Fig. S4. CG methylation near *A. thaliana* imprinted genes. Snapshots of CG methylation in indicated tissues near maternally expressed (red) and paternally expressed (blue) *A. thaliana* imprinted genes. Green bars represent embryo methylation, orange bars represent endosperm methylation, and red and blue bars represent methylation of the maternal and paternal genomes, respectively. Arrows point out methylation changes in endosperm and vegetative cell.

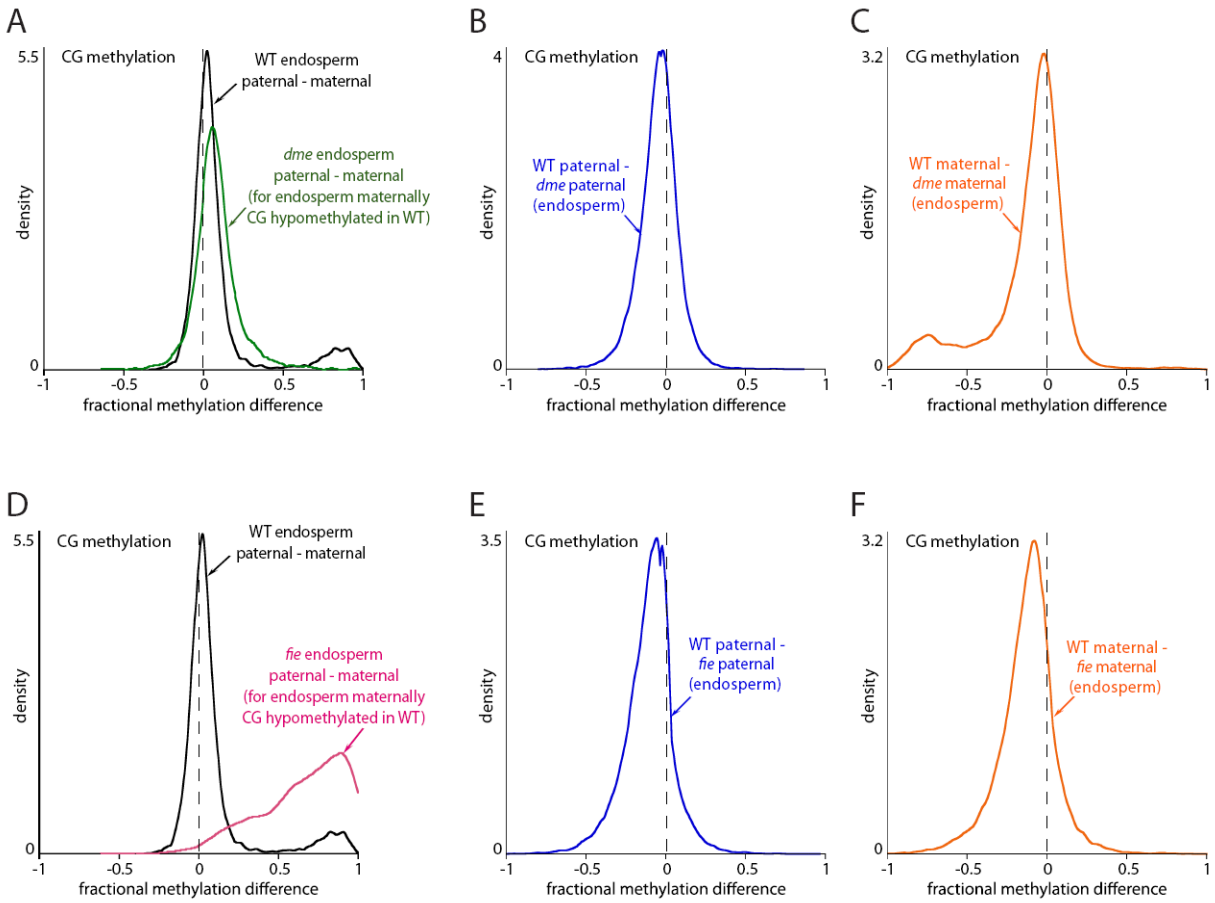

Fig. S5. DNA methylation in *dme* and *fie* endosperm. (**A-F**) Kernel density plots trace the frequency distribution of the *A. thaliana* CG methylation differences between the indicated endosperm genomes.

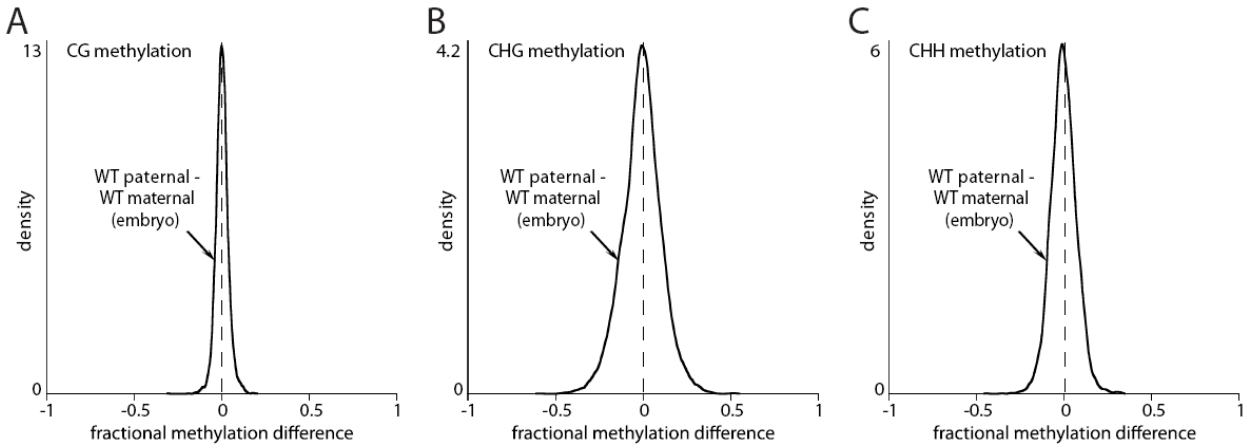

Fig. S6. DNA methylation in *A. thaliana* embryo. (**A-C**) Kernel density plots trace the frequency distribution of the differences between paternal and maternal embryo methylation in *A. thaliana*.

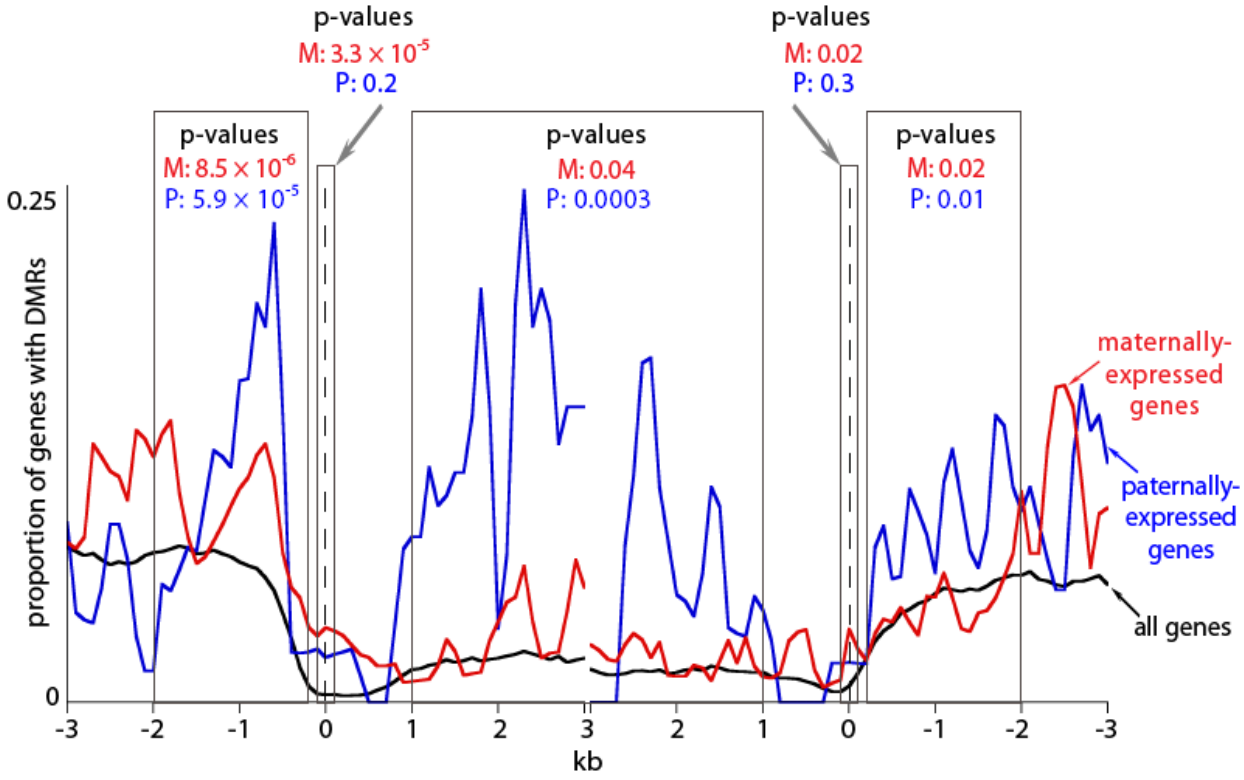

Fig. S7. Endosperm DNA demethylation near imprinted genes. Distribution of significantly differentially methylated regions between wild-type and *dme* mutant endosperm (DMRs) near *A. thaliana* genes. Genes were aligned at the 5' end (left dashed line) or the 3' end (right dashed line) and the proportion of genes with DMRs in each 100-bp interval is plotted. DMR distribution is shown with respect to maternally expressed imprinted genes (red trace), paternally expressed imprinted genes (blue trace) and all genes (black trace). Significance of DMR enrichment with respect to all genes (Fisher's exact test) for particular genic regions is shown in gray boxes.

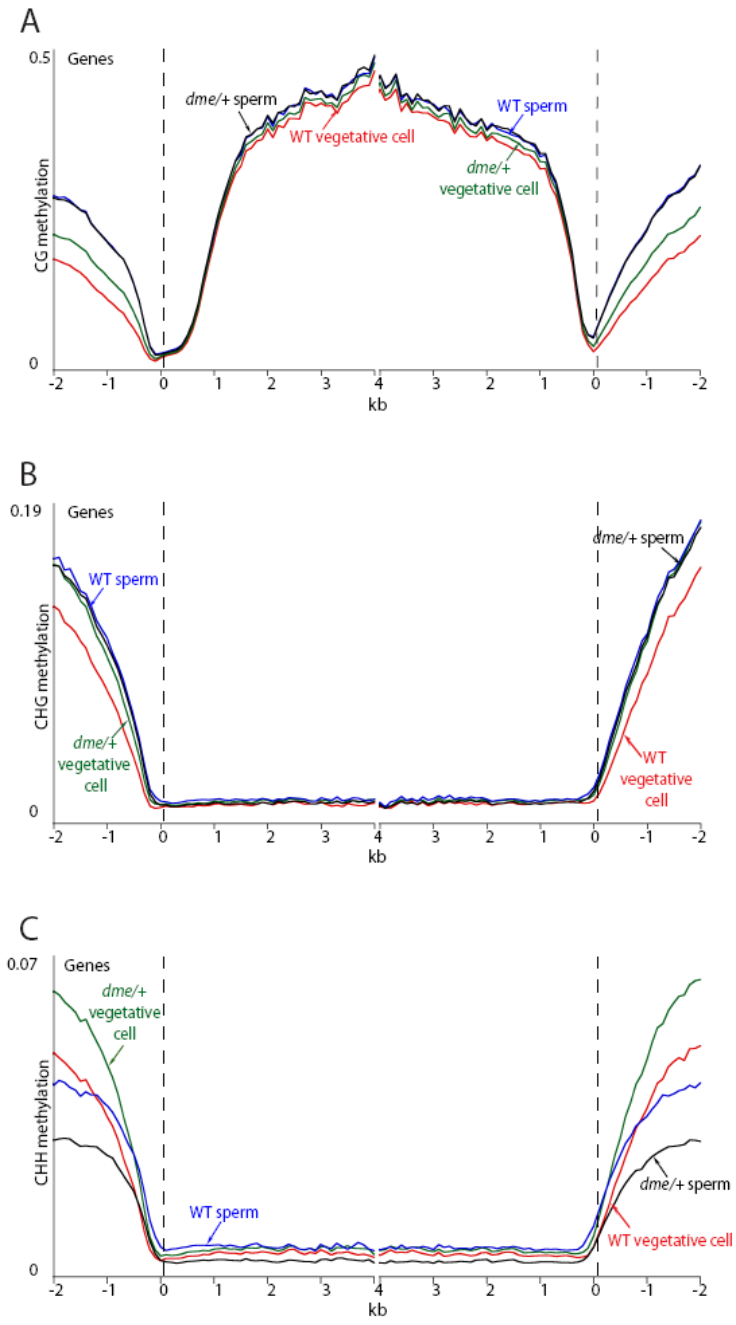

Fig. S8. Pollen DNA methylation in genes for wild-type and *dme-2*/+. (**A-C**) *A. thaliana* genes were aligned at the 5' end (left panel) or the 3' end (right panel) and average methylation levels for each 100-bp interval are plotted for vegetative and sperm cell genomes derived from wild-type and *dme-2*/+ pollen. The dashed line at zero represents the point of alignment. CG methylation is shown in (**A**), CHG in (**B**), CHH in (**C**). Note that WT vegetative cell CHG methylation is lower than sperm CHG methylation near genes (**B**) because small TEs that are preferentially demethylated by DME in vegetative cell nuclei cluster near genes (Fig. 3C). Likewise, CHH methylation in vegetative cells is lower than in sperm immediately adjacent to genes, but becomes higher than in sperm further from genes (**C**).

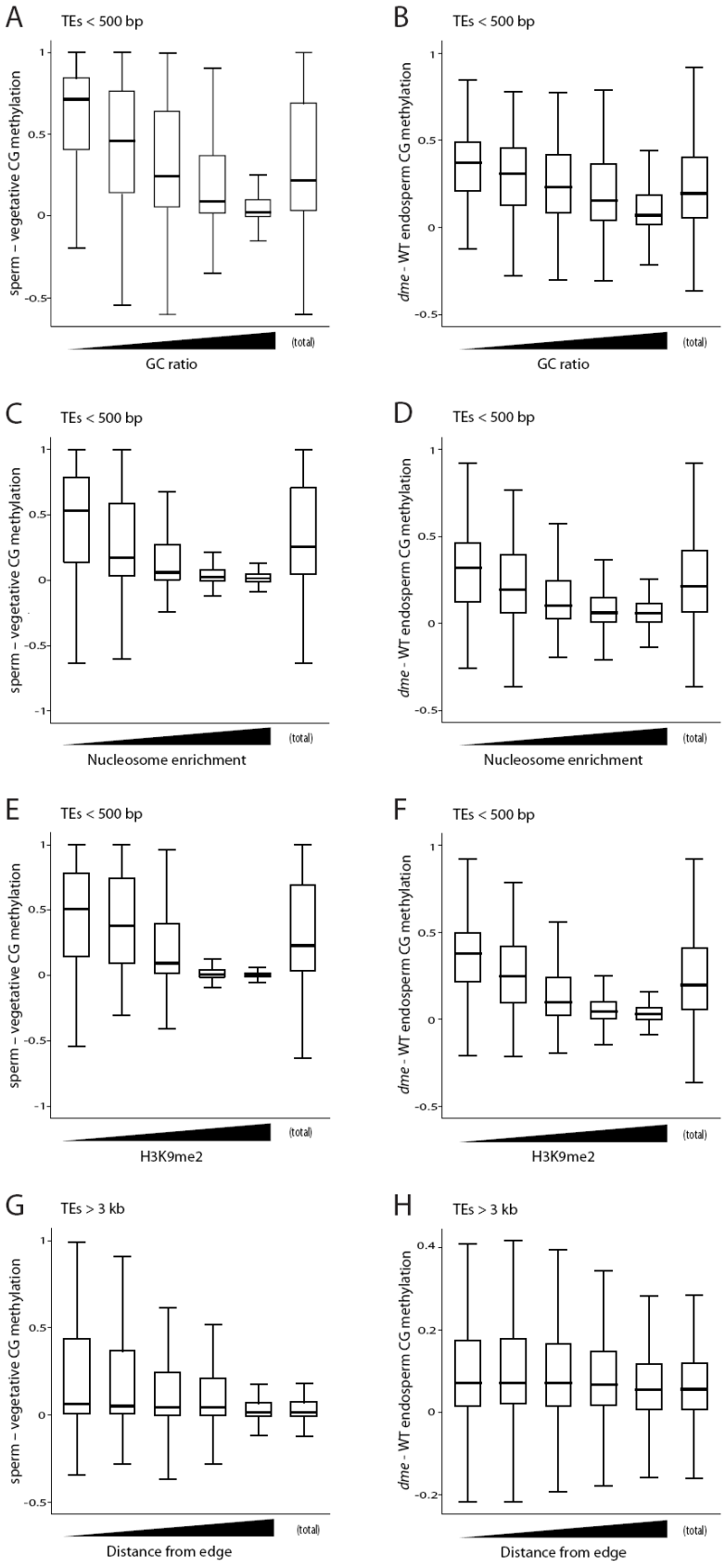

Fig. S9. DNA demethylation in transposons in relation to genomic features. (**A-H**) Box plots showing absolute fractional demethylation of 50-bp windows within transposons. Each box encloses the middle 50% of the distribution, with the horizontal line marking the median, and vertical lines marking the minimum and maximum values that fall within 1.5 times the height of the box. Differences between the first and the fifth categories from the left are significant for all panels ($p<0.001$, Kolmogorov-Smirnov test).

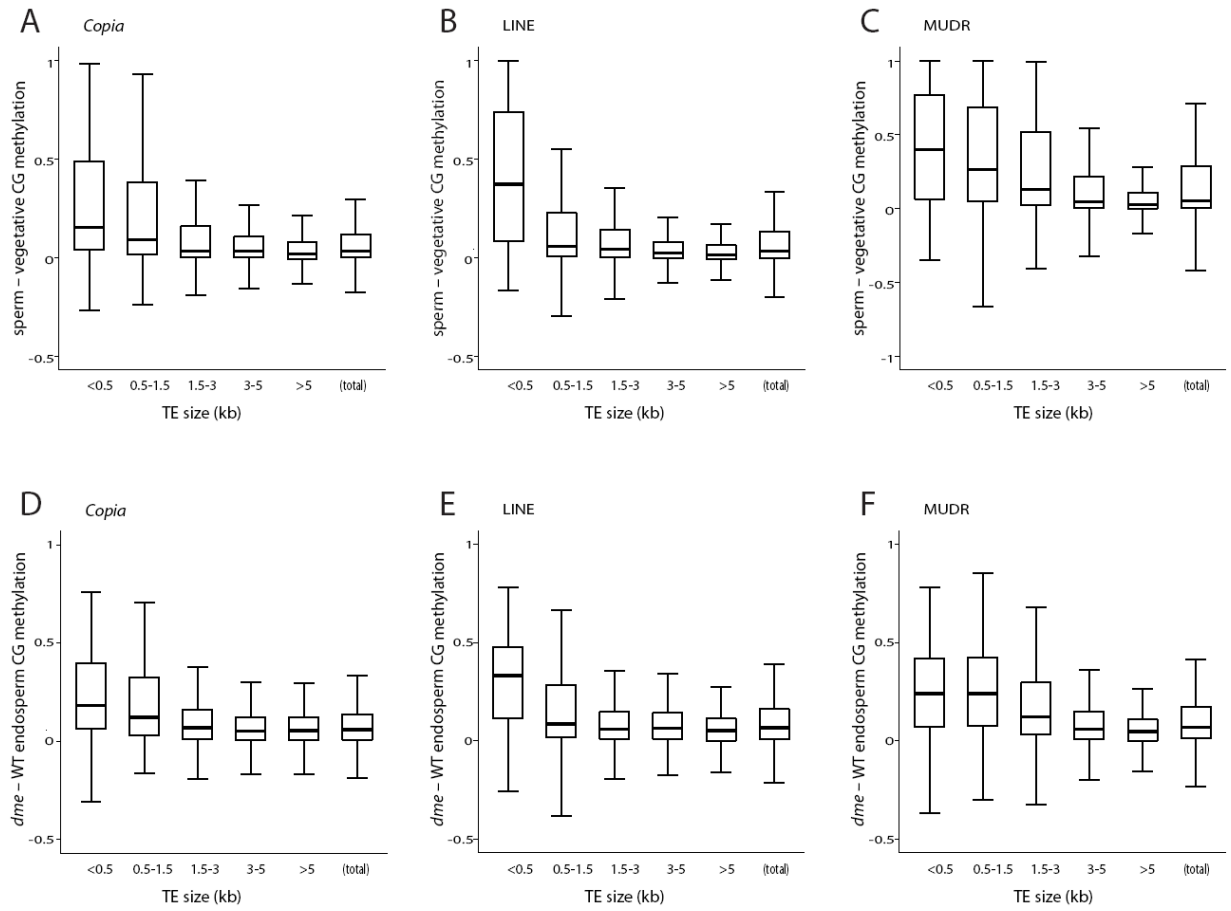

Fig. S10. Small TEs are preferentially demethylated regardless of type. (**A-F**) Box plots showing absolute fractional demethylation of 50-bp windows within three families of transposons: *Copia* (LTR retrotransposon), LINE (non-LTR retrotransposon) and MuDR (DNA transposon). Each box encloses the middle 50% of the distribution, with the horizontal line marking the median. The lines extending from each box mark the minimum and maximum values that fall within 1.5 times the height of the box. Sperm-vegetative differences are shown in (**A-C**) and *dme*-WT endosperm differences in (**D-F**). Differences between the first (<0.5 kb) and the fifth (>5 kb) categories are significant for all panels ($p<0.001$, Kolmogorov-Smirnov test).

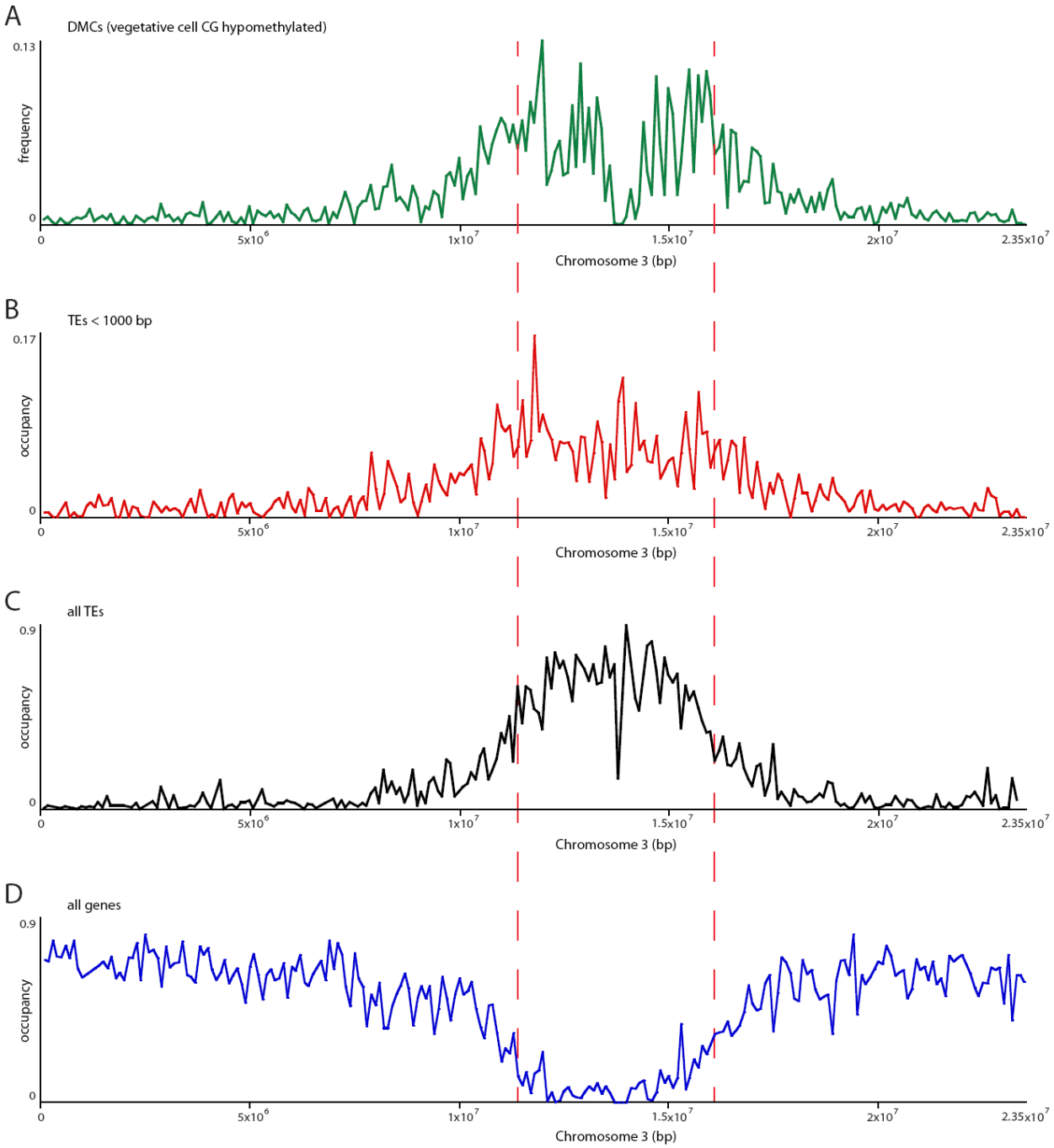

Fig. S11. Distribution of CG sites demethylated in vegetative nuclei. (**A-D**) Distribution across *A. thaliana* chromosome 3 of significantly differentially methylated cytosines (DMCs; p-value < 0.0001, Fisher's exact test) in the CG context that are less methylated in wild-type vegetative cells than in sperm (**A**), transposable elements smaller than 1 kb (**B**), all transposable elements (**C**), and genes (**D**). The dashed lines roughly mark the boundaries of pericentric heterochromatin.

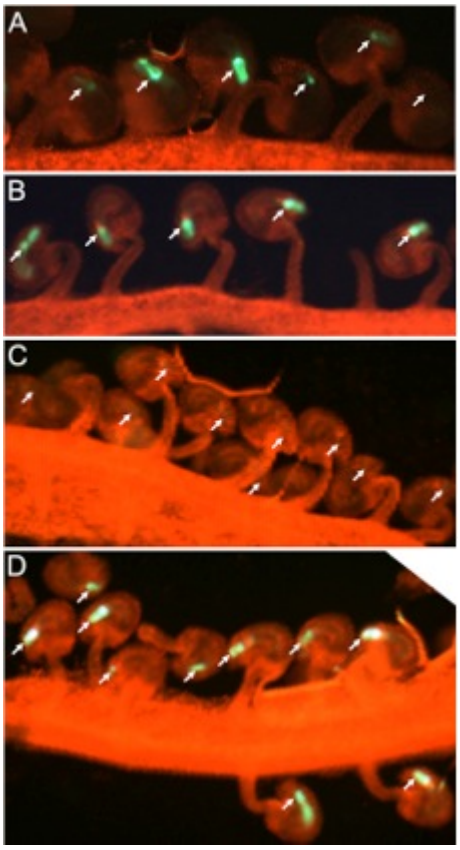

Fig. S12. An anti-GFP microRNA expressed in the central cell correlates with reduced GFP in the egg. To test whether sRNAs can travel from the central cell to the egg, we expressed a microRNA in the central cell that targets cleavage of *GFP* RNA expressed from a transgene in the egg. **(A)** Egg cell GFP expression in a primary transgenic line (table S5, line 2) hemizygous for a transgene expressing an anti-GFP microRNA in the central cell. **(B)** Egg cell GFP expression in a control primary transgenic line (table S5, line 7) lacking the microRNA. **(C)** Egg cell GFP expression that is nearly completely silenced in a plant that is the progeny of the line shown in (**A**) (table S5, line 2e). **(D)** Egg cell GFP expression that is not silenced in a plant that is the progeny of the line shown in (**A**) (table S5, line 2a). All lines are homozygous for the transgene that expresses *GFP* in the egg. Arrows point to egg cells. The promoter used for central cell-specific expression, *AGL61*, does not display detectable activity in the egg cell, or during early female gametophyte development prior to cellularization, when used by others (*24*). However, we cannot rule out the possibility of low-level expression of the anti-GFP microRNA prior to cellularization in the female gametophyte or in the egg cell in the independent transgenic lines we generated (table S5). Further experiments are required to determine whether 24-nt sRNA molecules that mediate DNA methylation are also able to move.

Sample	Median Coverage	Methylation (%) Nuclear CG	Nuclear CHG	Nuclear CHH	Chloroplast CHH	M/P ratio
Col x L*er* embryo	5	29.2	11.8	4.6	0.1	0.96
L*er* x Col embryo	11	29.6	12.1	5.1	0.1	0.93
Col x L*er* endosperm	20	23.7	8.7	3.4	0.4	1.99
L*er* x Col endosperm	29	22.6	8.6	3.0	0.1	1.95
dme-2 x L*er* endosperm	22	27.2	4.7	0.7	0.2	2.09
Col x *fie-1* endosperm	20	26.7	5.6	0.8	0.3	2.06
WT vegetative cell	33	26.9	13.0	4.0	0.3	NA
WT sperm cell	37	31.2	12.7	2.1	0.6	NA
dme-2/+ vegetative cell	45	28.7	14.1	4.7	0.3	NA
dme-2/+ sperm cell	40	31.0	12.4	1.5	0.3	NA

Table S1. Median coverage per cytosine and mean DNA methylation for the indicated samples. Chloroplast CHH methylation is a measure of cytosine non-conversion and other errors. M/P = maternal/paternal; the expected ratio is 1 for embryo and 2 for endosperm. NA = not applicable.

Tissue	Total number	Total bp covered	Minimum length (bp)	Maximum length (bp)	Average length (bp)	% overlap
endosperm	9,816	4,433,250	100	7,750	452	45.5
pollen	9,932	4,068,000	100	6,400	410	49.6

Table S2. Endosperm and pollen DMRs. Continuous differentially methylated regions (DMRs) for endosperm (using the difference between *dme* and WT endosperm) and pollen (using the difference between sperm and vegetative cell). % overlap for endosperm indicates percentage of sequence that overlaps with pollen DMRs, and for pollen indicates percentage of sequence that overlaps with endosperm DMRs.

Endosperm TE size (bp)	% of all demethylated loci	O/E for all loci	p-value for all loci	% of demethylated TE loci	O/E for TE loci	p-value for TE loci
< 500	11.7	3.34	3.4×10^{-43}	29.4	4.14	1.7×10^{-61}
< 1000	19.5	2.95	1.5×10^{-62}	49.1	3.65	2.6×10^{-100}
> 1000	20.2	0.48	9.5×10^{-80}	50.9	0.59	2.6×10^{-100}
> 3000	8.2	0.25	2.2×10^{-118}	20.5	0.31	1.2×10^{-118}

Vegetative cell TE size (bp)	% of all demethylated loci	O/E for all loci	p-value for all loci	% of demethylated TE loci	O/E for TE loci	p-value for TE loci
< 500	8.6	2.67	$< 10^{-299}$	15.8	2.41	$< 10^{-299}$
< 1000	19.4	2.73	$< 10^{-299}$	35.6	2.47	$< 10^{-299}$
> 1000	35.1	0.83	$< 10^{-299}$	64.4	0.75	$< 10^{-299}$
> 3000	14.5	0.46	$< 10^{-299}$	26.6	0.42	$< 10^{-299}$

Table S3. Small TEs are preferentially demethylated. Statistics for fractions of 50-bp windows demethylated in the maternal endosperm genome (top) or in the vegetative cell genome (bottom), as defined in the Materials and Methods for Fig. 1-2, that correspond to transposable elements of various lengths as a fraction of either all loci or of TE loci that are demethylated in the indicated tissue. O/E = observed/expected ratio. Probability values were calculated using Fisher's exact test. Please note that TE annotation is not comprehensive, so the reported TE fractions of total loci are likely underestimates of the actual TE fraction of total loci.

TE	Endosperm maternal/paternal transcript ratio	p-value	Sperm-vegetative cell DMR
AT4TE04415	256	1.60895E-15	Yes
AT4TE08130	69	2.70462E-06	Yes
AT2TE41175	57.33	2.97766E-06	Yes
AT4TE17660	52.36	3.09028E-13	Yes
AT2TE24245	32	0.009	Yes
AT3TE54360	28	0.02	Yes
AT2TE13520	19.33	0.013	Yes
AT3TE63935	18	0.001	Yes
AT5TE44975	15.33	0.028	Yes
AT2TE11110	15	0.015	Yes
AT3TE63215	14.57	0.003	Yes

Table S4. DME-dependent maternally expressed endosperm TEs. TEs specifically expressed from the maternal endosperm genome (Fisher's exact test p-value) that overlap a DME-mediated DMR (table S2) and that are not expressed in *dme* mutant endosperm. All TEs also overlap a sperm-vegetative cell DMR (table S2).

Line	Transgene	No or faint GFP	Strong GFP	N	% GFP	χ^2 (1:1)	P
1	*AGL61p-amiRNA=GFP*	118	102	220	46	1.16	> 0.28
2		106	96	202	48	0.50	> 0.48
3		100	81	181	45	1.99	> 0.16
4		104	112	216	52	0.30	> 0.59
5		105	107	212	50	0.02	> 0.89
6	*AGL61p*	14	199	213	93	-	-
7		16	202	218	93	-	-
8		7	210	217	97	-	-
9		14	201	215	93	-	-
10		16	216	232	93	-	-
11		22	171	193	89	-	-
12		21	205	226	91	-	-
13		15	207	222	93	-	-
14	*DD45p-amiRNA=GFP*	65	50	115	44	2	> 0.16
15		84	130	214	60	10	> 0.002
16		97	105	202	52	0.3	> 0.57
2a	*Line 2, backcrossed & selfed*	30	148	178	83	78	> 0.0001
2b		33	26	59	44	0.83	> 0.36
2c		36	31	67	46	0.37	> 0.54
2d		112	15	127	12	74	> 0.0001
2e		79	7	86	8	60	> 0.0001

Table S5. The indicated transgenes were introduced into lines homozygous for the *DD45p-GFP* reporter gene that expresses *GFP* in the egg cell (*25*). Lines 1-16 represent independent transgenic events. The *AGL61p-amiRNA=GFP* silencer transgene specifically expresses in the central cell (*24*) an artificial microRNA that targets *GFP* RNA. The *AGL61p* transgene is a negative control. The *DD45p-amiRNA=GFP* transgene is a positive control that specifically expresses in the egg cell (*25*) the artificial microRNA that targets GFP RNA. After meiosis, a single hemizygous transgene in the primary T1 line is inherited by 50% of the female gametophytes. If the transgene silences the *DD45p-GFP* reporter, we expect to detect 50% of the egg cells with strong GFP fluorescence and 50% of the egg cells with faint or no GFP fluorescence. We observed this result in lines 1-5 that are hemizygous for the silencer transgene. The same result was observed in the positive control lines 14-16, but not in the negative control transgenic lines 6-13. We analyzed the segregation of the silencer transgene in subsequent generations. Line 2 was backcrossed to a plant homozygous for the *DD45p-GFP* reporter gene. A hemizygous plant from the backcross was self-pollinated and GFP fluorescence in egg cells from progeny (lines 2a-2e) was analyzed. In lines 2d and 2e, most egg cells did not display GFP fluorescence. In lines 2b and 2c, approximately 50% of ovules displayed egg cells with GFP fluorescence. In line 2a, nearly all egg cells displayed GFP fluorescence. N, number of egg cells examined. % GFP, percentage of egg cells with strong GFP fluorescence. χ^2, calculated for a 1:1 segregation of egg cells with no or faint GFP fluorescence versus strong GFP fluorescence. P, probability that the deviation from the expected 1:1 segregation is due to chance.

References and Notes

1. J. A. Law, S. E. Jacobsen, Establishing, maintaining and modifying DNA methylation patterns in plants and animals. *Nat. Rev. Genet.* **11**, 204 (2010).

2. M. J. Bauer, R. L. Fischer, Genome demethylation and imprinting in the endosperm. *Curr. Opin. Plant Biol.* **14**, 162 (2011).

3. T.-F. Hsieh *et al*., Genome-wide demethylation of *Arabidopsis* endosperm. *Science* **324**, 1451 (2009).

4. T.-F. Hsieh *et al*., Regulation of imprinted gene expression in *Arabidopsis* endosperm. *Proc. Natl. Acad. Sci. U.S.A.* **108**, 1755 (2011).

5. Materials and methods are available as supporting material on *Science Online*.

6. M. Gehring *et al*., DEMETER DNA glycosylase establishes *MEDEA* Polycomb gene self-imprinting by allele-specific demethylation. *Cell* **124**, 495 (2006).

7. R. K. Slotkin *et al*., Epigenetic reprogramming and small RNA silencing of transposable elements in pollen. *Cell* **136**, 461 (2009).

8. V. K. Schoft *et al*., Function of the DEMETER DNA glycosylase in the *Arabidopsis thaliana* male gametophyte. *Proc. Natl. Acad. Sci. U.S.A.* **108**, 8042 (2011).

9. V. K. Schoft *et al*., Induction of RNA-directed DNA methylation upon decondensation of constitutive heterochromatin. *EMBO Rep.* **10**, 1015 (2009).

10. F. Roudier *et al*., Integrative epigenomic mapping defines four main chromatin states in *Arabidopsis*. *EMBO J.* **30**, 1928 (2011).

11. W. Qian *et al*., A histone acetyltransferase regulates active DNA demethylation in *Arabidopsis*. *Science* **336**, 1445 (2012).

12. M. Pillot *et al*., Embryo and endosperm inherit distinct chromatin and transcriptional states from the female gametes in *Arabidopsis*. *Plant Cell* **22**, 307 (2010).

13. A. Zemach *et al*., Local DNA hypomethylation activates genes in rice endosperm. *Proc. Natl. Acad. Sci. U.S.A.* **107**, 18729 (2010).

14. R. Lister *et al*., Highly integrated single-base resolution maps of the epigenome in *Arabidopsis*. *Cell* **133**, 523 (2008).

15. J. Penterman *et al*., DNA demethylation in the *Arabidopsis* genome. *Proc. Natl. Acad. Sci. U.S.A.* **104**, 6752 (2007).

16. Y. Choi *et al*., DEMETER, a DNA glycosylase domain protein, is required for endosperm gene imprinting and seed viability in *Arabidopsis*. *Cell* **110**, 33 (2002).

17. N. Ohad *et al*., Mutations in *FIE*, a WD Polycomb group gene, allow endosperm development without fertilization. *Plant Cell* **11**, 407 (1999).

18. A. Zemach, I. E. McDaniel, P. Silva, D. Zilberman, Genome-wide evolutionary analysis of eukaryotic DNA methylation. *Science* **328**, 916 (2010).

19. R. K. Chodavarapu *et al*., Relationship between nucleosome positioning and DNA methylation. *Nature* **466**, 388 (2010).

20. Y. V. Bernatavichute, X. Zhang, S. Cokus, M. Pellegrini, S. E. Jacobsen, Genome-wide association of histone H3 lysine nine methylation with CHG DNA methylation in *Arabidopsis thaliana*. *PLoS ONE* **3**, e3156 (2008).

21. S. Y. Kim, J. Lee, L. Eshed-Williams, D. Zilberman, Z. R. Sung, EMF1 and PRC2 cooperate to repress key regulators of *Arabidopsis* development. *PLoS Genet.* **8**, e1002512 (2012).

22. P. Wolff *et al*., High-resolution analysis of parent-of-origin allelic expression in the Arabidopsis endosperm. *PLoS Genet.* **7**, e1002126 (2011).

23. M. Gehring, V. Missirian, S. Henikoff, Genomic analysis of parent-of-origin allelic expression in *Arabidopsis thaliana* seeds. *PLoS ONE* **6**, e23687 (2011).

24. J. G. Steffen, I. H. Kang, M. F. Portereiko, A. Lloyd, G. N. Drews, AGL61 interacts with AGL80 and is required for central cell development in Arabidopsis. *Plant Physiol.* **148**, 259 (2008).

25. J. G. Steffen, I.-H. Kang, J. Macfarlane, G. N. Drews, Identification of genes expressed in the Arabidopsis female gametophyte. *Plant J.* **51**, 281 (2007).

26. K. S. Century *et al*., NDR1, a pathogen-induced component required for *Arabidopsis* disease resistance. *Science* **278**, 1963 (1997).

27. D. R. Smyth, J. L. Bowman, E. M. Meyerowitz, Early flower development in *Arabidopsis*. *Plant Cell* **2**, 755 (1990).

28. R. Yadegari *et al*., Mutations in the FIE and MEA genes that encode interacting Polycomb proteins cause parent-of-origin effects on seed development by distinct mechanisms. *Plant Cell* **12**, 2367 (2000).